

Thermal decomposition of $[\text{Co}(\text{NH}_3)_6]_2(\text{C}_2\text{O}_4)_3 \cdot 4\text{H}_2\text{O}$ II. Identification of the gaseous products

Ewa Ingier-Stocka^a, Marek Maciejewski^{b,*}

^a *Institute of Inorganic Chemistry and Metallurgy of Rare Elements, Wrocław University of Technology,
Wybrzeże St. Wyspińskiego 27, PL 50-370 Wrocław, Poland*

^b *Institute of Chemical and Bioengineering, Swiss Federal Institute of Technology, ETH-Hoenggerberg,
ICB, HCI E139, CH-8093 Zurich, Switzerland*

Received 2 June 2004; received in revised form 6 August 2004; accepted 6 August 2004

Available online 25 April 2005

Abstract

The main goal of the presented work was to verify the previously assumed decomposition stages of $[\text{Co}(\text{NH}_3)_6]_2(\text{C}_2\text{O}_4)_3 \cdot 4\text{H}_2\text{O}$ (HACOT) [Thermochim. Acta 354 (2000) 45] under different atmospheres (inert, oxidising and reducing). The gaseous products of the decomposition were qualitatively and quantitatively analysed by mass spectrometry (MS) and Fourier-transformed infrared spectroscopy (FT-IR). It was confirmed that the gaseous products of HACOT decomposition under studied atmospheres there were H_2O (stage I) and NH_3 , CO_2 (stage II). The main gaseous products in the third stage in argon and hydrogen (20 vol.% H_2/Ar) were CO and CO_2 , whereas in air (20 vol.% O_2/Ar) only CO_2 was identified. Under the oxidising as well as reducing atmospheres the influence of secondary reactions on the composition of both, solid and gaseous products was found particularly strong during the third stage of the process. The studies of the multistage decomposition of HACOT, additionally complicated by many secondary reactions, required application of the hyphenated TA–MS or TA–FT-IR techniques combined with the pulse thermal analysis PTA[®] allowing quantification of the spectroscopic signals and investigation of gas–solid and gas–gas reactions in situ.

© 2004 Elsevier B.V. All rights reserved.

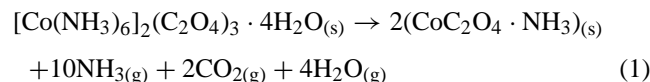
Keywords: Hexaaminecobalt(III) oxalate tetrahydrate; Thermal decomposition; Hyphenated techniques in thermal analysis; Pulse thermal analysis; Mass spectrometry

1. Introduction

The present work is the second part of our studies to determine the course of thermal decomposition of hexaaminecobalt(III) oxalate tetrahydrate (HACOT) [1]. Due to the multistage character of the decomposition and possibility of many secondary gas–solid and gas–gas reactions the identification of the mechanism of its decomposition is very difficult. The proposed method of interpretation and quantification of the mass spectrometric results can be used as an illustration of the elaboration of multicomponent MS traces.

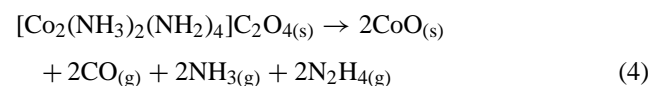
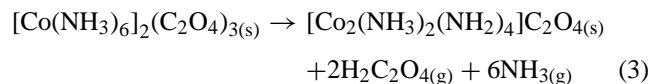
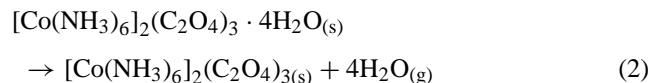
Among numerous publications (see a survey in Refs. [2–4]) relating to the thermal decomposition of cobalt

aminecomplexes only two of them are devoted to the thermal decomposition of HACOT, i.e. a part of Hadrich's dissertation [5] and an article by Jeyaraj and House [6]. The results and conclusions published in these works are contradictory. Hadrich [5] investigated dissociation of HACOT in different gas atmospheres using TG, DTG, DTA and EGA (mass spectrometry in vacuum) methods. He stated that the process occurred in three stages and suggested that the compound with the stoichiometric formula $\text{CoC}_2\text{O}_4 \cdot x\text{NH}_3 \cdot y\text{H}_2\text{O}$ (where $x + y = 1$) as an intermediate of the second stage of decomposition. The following overall reaction for slightly separated the first and second stages was proposed:



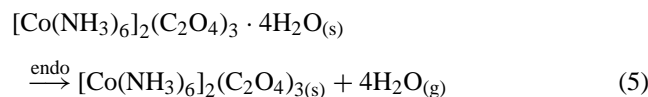
* Corresponding author. Tel.: +41 1 632 7836; fax: +41 1 632 1163.
E-mail address: maciejewski@chem.ethz.ch (M. Maciejewski).

Jeyaraj and House [6] studied the thermal decomposition of HACOT in a dynamic nitrogen atmosphere using TG–DTG methods. To identify the solid products of dissociation they carried out the chemical and infrared analysis. Likewise Hadrich, they consider the decomposition of HACOT occurs in three steps and suggest that the course of the reaction is expressed by Eqs. (2)–(4):

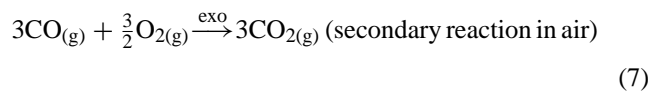
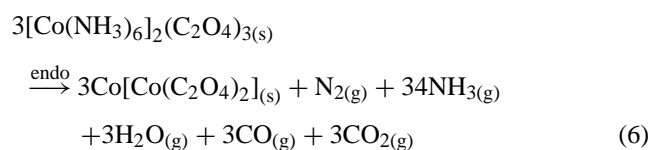


The authors of the present work studied thermal decomposition of HACOT in air and argon atmospheres under non-isothermal, isothermal and quasi-isothermal-isobaric conditions [1]. Identification of intermediates and final products in solid phase was carried out using spectroscopy (Far-IR, IR, UV–vis), magnetic susceptibility and X-ray diffraction. The dissociation of HACOT was found to occur in three stages in both gas atmospheres and the following sequences of the reaction stages in non-isothermal and isothermal conditions were proposed [1]:

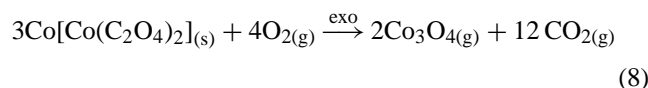
Stage I (air, argon):



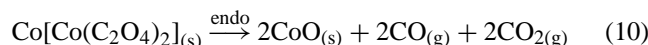
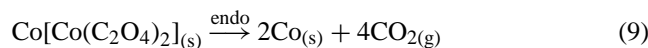
Stage II (air, argon):



Stage III (air):

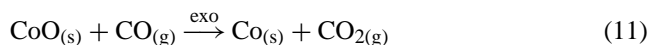


Stage III (argon):



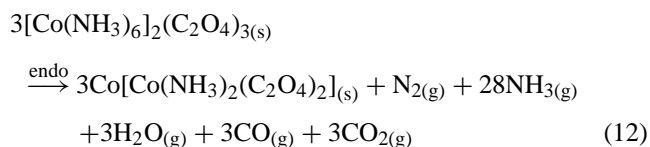
Reactions (9) and (10) can proceed in parallel.

A combination of (10) and secondary reaction (11) cannot also be excluded:



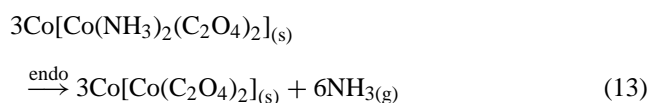
It was assumed that the substages of complex stage II may be expressed by means of the reactions (12)–(14):

Substage IIa (air, argon):

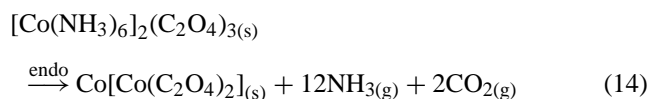


and reaction (7)

Substage IIb (air, argon):



On the basis of some literature data related to aminocomplexes decomposition, e.g. [2,7] it has been assumed that the agent reducing Co(III) to Co(II) is ammonia. Taking into account that this conclusion was drawn from the analysis of the solid products of the decomposition only this assumption cannot be proved explicitly. Also a hypothesis about oxalate ions as the reducing agent cannot be excluded as well. Then the overall reaction for the stage II would proceed according to Eq. (14):



The verification of the assumed decomposition stages is possible only on the basis of the investigation of gas products composition.

It was stated in our former work [1] that the solid intermediate after the second stage of decomposition of HACOT was $\text{Co}[\text{Co}(\text{C}_2\text{O}_4)_2]$ (see Eqs. (6), (13) and (14)). A survey of a literature concerning of cobalt oxalate dihydrate (COD) decomposition published in Ref. [8] shows many controversial opinions concerning the mechanism of this reaction. The controversy over the solid products of COD decomposition in particular gas atmospheres concerns especially the reaction course in an inert atmosphere. In our studies of thermal dissociation of COD using TA–MS–PTA[®] technique [8] the composition of the solid and gaseous products as well as heat of dehydration and decomposition of oxalate were determined in inert, oxidising and hydrogen-containing atmospheres. Contrary to the previous suggestions about the mechanism of COD decomposition, it was stated the solid product formed during decomposition in helium contained not only metallic Co_{met} but also a substantial amount of CoO (ca. 13 mol.%). Moreover, the composition of the primary

solid and gaseous products changes in all atmospheres as a result of secondary gas–solid and gas–gas reactions, catalysed by freshly formed Co_{met} . The results presented in [8] clearly indicate that an interpretation of a complex mechanism of decomposition of solids based only on the TG–DTG–DTA signals could be sometimes of little value. Mass change alone does not allow for deeper insight into all of the potential primary and secondary reactions that could occur. The observed mass changes (TG) and thermal effects (DTA/DSC) are a superposition of several phenomena and thus do not necessarily reflect the solid substrate decomposition alone. Investigation of the mechanism of decomposition requires the application of different simultaneous techniques that allow the qualitative and quantitative determination of the gaseous products of the decomposition.

The main goal of the presented work was to verify the assumed decomposition stages by applying qualitative and quantitative analysis of gaseous products by mass spectrometry (MS) and Fourier-transformed infrared spectroscopy (FT-IR).

2. Experimental

The simultaneous technique thermal analysis–mass spectrometry–pulse thermal analysis (TA–MS–PTA[®]) was used. Experiments were carried out with a Netzsch STA 409 simultaneous thermal analyser equipped with a gas pulse device that enables the injection of controlled amounts of one or two different pure gases or gaseous mixtures into the carrier gas stream. The thermal analyser was coupled via a heated capillary with a Balzers QMG 420 quadrupole mass spectrometer. The decompositions were carried out under inert (Ar), oxidising (20 vol.% O_2 , balance Ar) and reducing atmospheres (20 vol.% H_2 , balance Ar). An exact flow of 50 ml min^{-1} was achieved using mass-flow controllers (Brooks model 5850E). The TG curves for each atmosphere were corrected to minimise the buoyancy effect by subtracting the TG base line obtained with the empty crucibles.

The injection of 1 ml pulses of CO , CO_2 , N_2 , H_2 and NH_3 (2 ml pulses) into the carrier gas stream enabled the quantification of the mass spectrometric curves recorded during the decomposition. Details of this procedure are given in [9,10].

The thermal decomposition experiments were carried out under non-isothermal conditions with heating rate $\beta = 5 \text{ K min}^{-1}$ between 25–500 °C. The sample mass was $72.4 \pm 0.1 \text{ mg}$. Three different types of crucibles were used, i.e. platinum (Pt), alumina (Alox) and quartz (Q) for the specimen and/or reference ($\alpha\text{-Al}_2\text{O}_3$).

Fourier transformed infrared spectroscopy (FT-IR) studies of gaseous products of decomposition in helium were carried out with a Bruker Vector 22 FT-IR spectrometer connected by a heated capillary with a thermoanalyzer STA 449C (Netzsch). The title compound $[\text{Co}(\text{NH}_3)_6]_2(\text{C}_2\text{O}_4)_3 \cdot 4\text{H}_2\text{O}$ (HACOT) was synthesised by the method described in [11].

The composition of the substrate was confirmed by elemental analysis and atomic absorption spectroscopy (AAS). The determined composition was Co: 18.21% found, 17.93% calc.; H: 6.97% found, 6.73% calc.; C: 11.95% found, 10.94% calc.; N: 24.13% found, 25.53% calc.

3. Results

The TA and MS signals obtained during decomposition of HACOT under different atmospheres are presented in figures as follows: in argon (Figs. 1, 2 and 6), in 20 vol.% H_2 , balance argon (Figs. 3 and 7) and in 20 vol.% O_2 , balance argon (Figs. 4 and 8). Figs. 5 and 9 illustrate the influence of different gas atmospheres on the course of the thermal decomposition of the title compound in platinum and quartz crucibles, respectively. Fig. 10 shows how the type of the crucible influences the dissociation of HACOT in argon atmosphere. Figs. 11 and 12 depict the influence of the crucible material on the CO conversion and behaviour of NH_3 in inert and oxidising atmosphere, respectively.

3.1. TG–DTA

The thermoanalytical results (thermogravimetry and differential thermal analysis) are summarised in Table 1. The thermal decomposition of HACOT proceeds in three stages, independently of the gas atmosphere. In the reducing

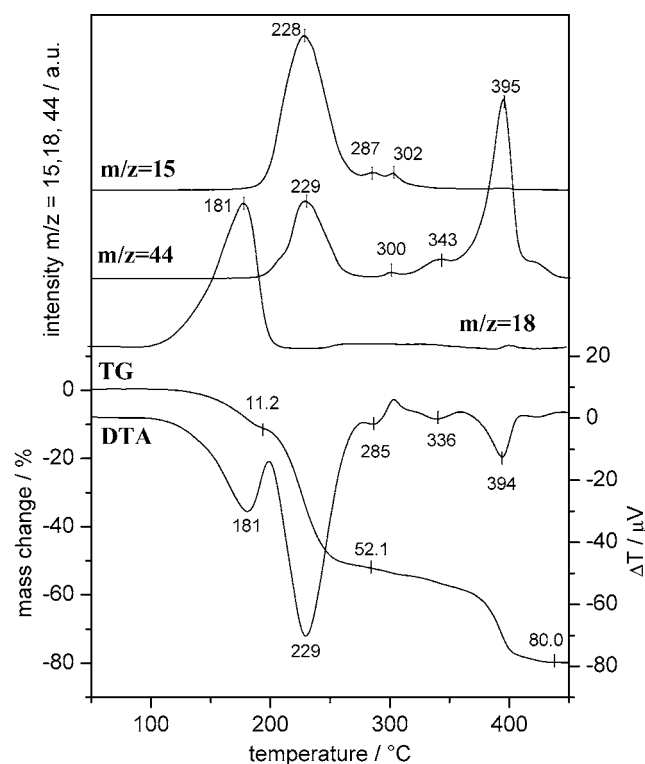


Fig. 1. Decomposition of $[\text{Co}(\text{NH}_3)_6]_2(\text{C}_2\text{O}_4)_3 \cdot 4\text{H}_2\text{O}$ in argon, platinum crucible.

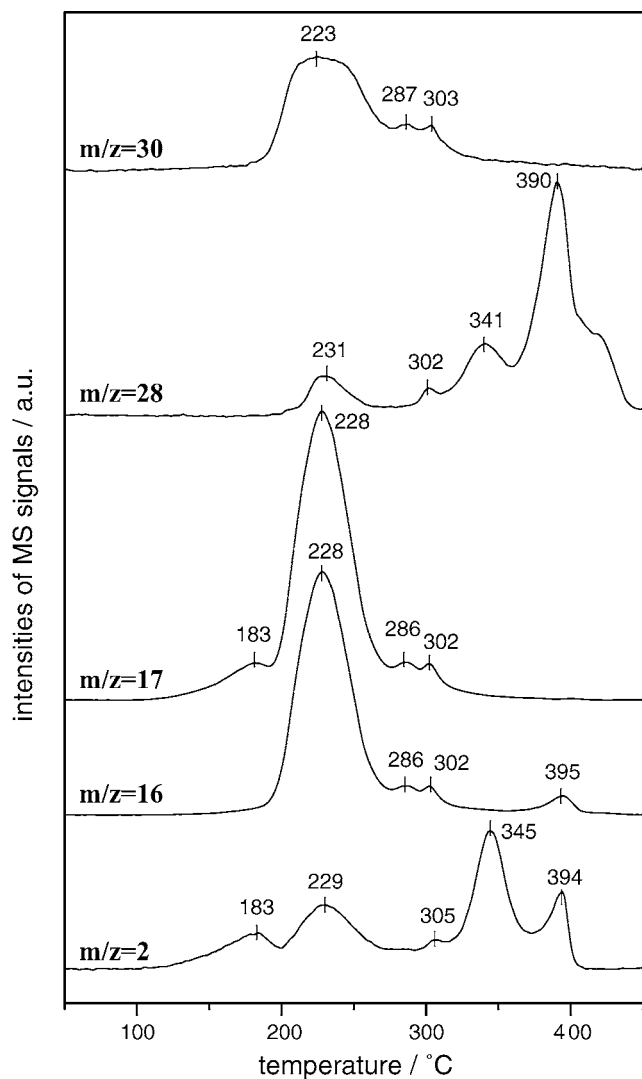


Fig. 2. Decomposition of $[\text{Co}(\text{NH}_3)_6]_2(\text{C}_2\text{O}_4)_3 \cdot 4\text{H}_2\text{O}$ in argon, platinum crucible, additional MS signals.

atmosphere the first and second stages are endothermic similar as in inert and oxidising atmospheres. In the third stage, both, endothermic and exothermic effects are observed. The temperature range and mass losses for the stages I and II were closed to each other in all atmospheres while they depend significantly on the atmosphere during the third stage. The solid final products of HACOT decomposition in argon and air were identified earlier [1] as a mixture of $\text{Co} + \text{CoO}$ (about 50 mol.%) and Co_3O_4 , respectively. It was also revealed previously that the residue of $\text{CoC}_2\text{O}_4 \cdot 2\text{H}_2\text{O}$ decomposition in the reducing atmosphere (20 vol.% H_2) was Co_{met} [8]. The formation of cobalt oxalate as the intermediate after the second stage of HACOT decomposition was already suggested in [1]. The mass loss observed in the reducing atmosphere (Table 1) is lower by ca. 1% than the stoichiometric value by the assumption that Co_{met} is the one solid product. This difference is due to the CO disproportionation catalysed by the metallic cobalt. The observed mass loss is influenced by

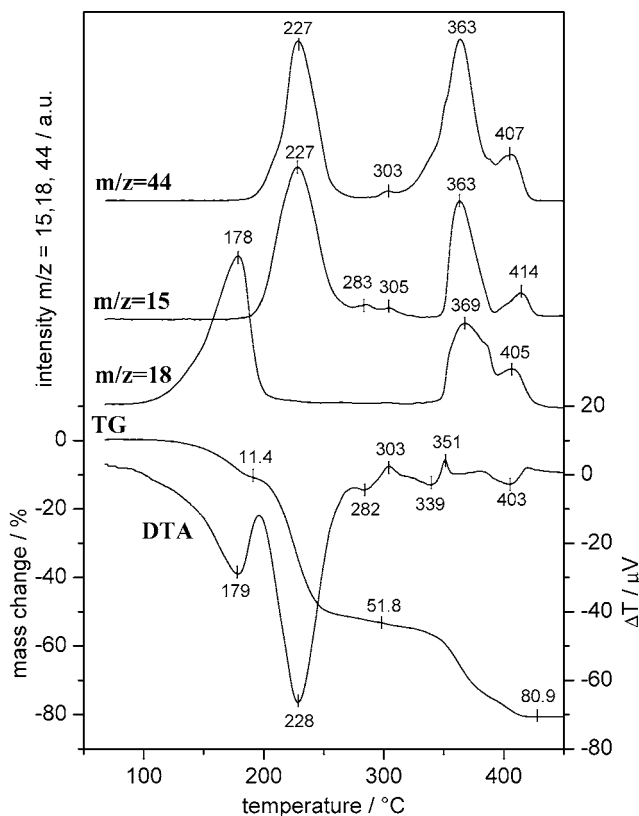


Fig. 3. Decomposition of $[\text{Co}(\text{NH}_3)_6]_2(\text{C}_2\text{O}_4)_3 \cdot 4\text{H}_2\text{O}$ in hydrogen (20 vol.%, balance Ar), platinum crucible.

the formation of carbon, the solid product of CO disproportionation (Table 2, Eq. (25)) as it was proven previously [8].

Discussing the phase ratio of the solid products $\text{Co}_{\text{met}}-\text{CoO}$ formed in the primary reaction of HACOT decomposition in an inert atmosphere it is necessary to take into account the possible decomposition and redox reactions (see Table 2, Eqs. (7), (10), (11) and (12)). The composition of the residue may be altered not only by secondary reactions with the carrier gas as happens with oxygen (oxidation of both solid products to Co_3O_4) and hydrogen (reduction of CoO to Co_{met}). It may be changed by the gas–solid reaction with the decomposition gaseous products as well. The CoO reacts with CO (the primary product of HACOT decomposition—Table 2, Eq. (6) and also, in lower extent, with H_2 or hydrocarbons formed during the decomposition. All these reaction were proved during decomposition of COD [8].

Due to the rapid oxidation of the metallic cobalt formed during HACOT decomposition in an inert atmosphere the determination of the composition of the solid products can be carried out only in situ, immediately after completing the decomposition. This procedure is illustrated by the results shown in the inset of Fig. 6. The reduction of the primary CoO was done by the injection of 1 ml pulses of hydrogen into the carrier gas stream (Ar) just after the HACOT decomposition was completed. Three hydrogen pulses were required for the total reduction of the CoO present in the residue (mass

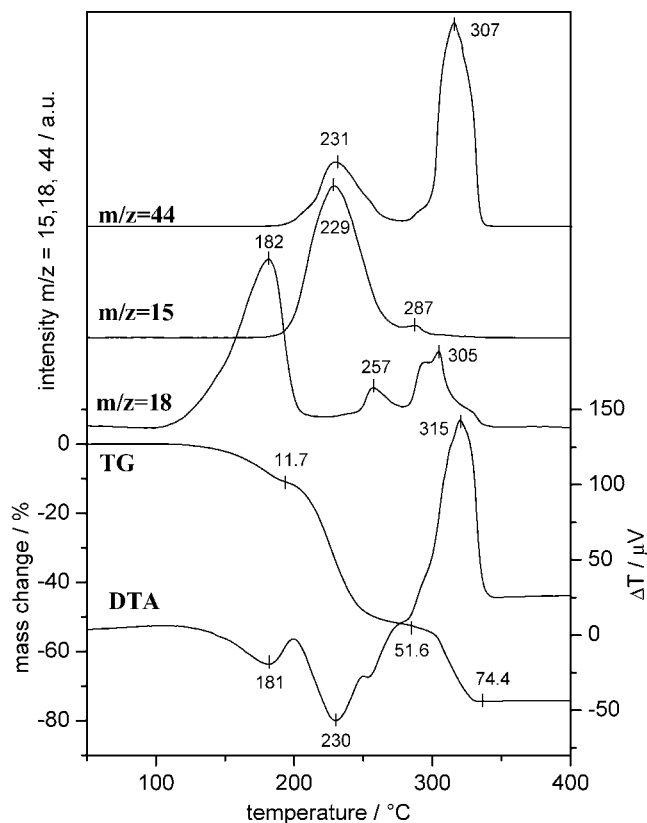


Fig. 4. Decomposition of $[\text{Co}(\text{NH}_3)_6]_2(\text{C}_2\text{O}_4)_3 \cdot 4\text{H}_2\text{O}$ in oxygen (20 vol.%, balance Ar), platinum crucible.

loss 1.025 mg, sample mass of HACOT 72.4 mg). Beside the main phase, Co_{met} , the solid residue contains 32.2 wt.% of CoO , which is equivalent to 27.2 mol%. The mass loss due to the CoO reduction amounts to 1.4 wt.% what summarised with that recorded at HACOT decomposition (79.7 wt.%) results in 81.1%—exactly the same as that recorded during HACOT decomposition in H_2 atmosphere when Co_{met} is the only product.

3.2. Gaseous products—qualitative mass spectrometric analysis

In the temperature range of the first stage of the decomposition, independent of the atmosphere, only water ($m/z = 18$; 17) was detected (Figs. 1–8). The temperatures of the maxima of MS spectra were similar, ca. 180 °C (Figs. 1, 3 and 4). The absence of other MS signals confirms that only dehydration equation (5) occurs during the first stage of the HACOT decomposition. However before the dehydration is completed the intensity of MS signals $m/z = 15$ and 44 starts to increase what points out the beginning of the second stage of the decomposition.

In the second stage of the HACOT decomposition independently of the crucible type and the gas atmosphere, the MS signals with $m/z = 15$, 16, 17, 28 and 44 are observed. They result from the primary gaseous products of HACOT

decomposition, i.e. NH_3 and CO_2 , respectively (see Figs. 1–10). However one ought to remember that the signal $m/z = 28$ may originate not only from CO_2 fragmentation (CO^+) but also from the presence of CO and N_2 as it was assumed in Eqs. (6) and (12). Only quantitative interpretation (PTA[®]–MS) of the MS curves, which is presented below, can help in solving the mechanism of the second stage of HACOT decomposition. The temperatures of the maxima of all these signals are very close to the temperature of the DTA peak, i.e. ca. 230 °C.

Figs. 5 and 9 illustrate the influence of the oxidising atmosphere on the second stage of the decomposition. On the MS curve $m/z = 18$ the additional peaks at 257 and 305 °C are observed (Pt crucible, Fig. 5) and at 289 °C (quartz crucible, Fig. 9). Also on the curve $m/z = 28$ (Pt crucible, Fig. 5) a small additional peak, not observed during the decomposition in the quartz crucible, is observed at 254 °C what suggests oxidation NH_3 to N_2 catalysed by the platinum. Within the range of temperatures characteristic for II and the beginning of III stage of decomposition (180–350 °C) in the oxidation atmosphere NH_3 is oxidised to N_2 , N_2O and NO (Table 2, Eqs. (17)–(19)) as it was confirmed by the reference tests with pure NH_3 (see Fig. 12) in which pulses of NH_3 were injected between RT and 750 °C in different atmospheres over different empty crucibles. As it can be seen platinum catalyses the process of NH_3 oxidation. Over Co_{met} ammonia starts to decompose at ca. 290 °C what is manifested by formation of hydrogen (not shown).

The MS curves shown in Figs. 5, 9 and 10 indicate that the atmosphere and material of crucible influence the course of the third stage very strongly. In oxidising atmosphere there is a very clear increase in intensity of the signal $m/z = 44$ in both, the Pt (Fig. 5, temperature 307 °C) as well as the quartz crucibles (Fig. 9, temperature 289 °C) in comparison to argon atmosphere. It is connected with oxidising of primary CO to CO_2 . In reducing atmosphere additional maxima on the curves $m/z = 18$ and 15 are observed at ca. 370 °C (Pt crucible – Fig. 5) and 334 °C, 364 and 376 °C (quartz crucible, Fig. 9). These temperatures are similar to the temperatures of peaks on the curves $m/z = 28$ and 44 (evolution of CO and CO_2 during HACOT decomposition) what confirms suggestion of the formation of methane and water in secondary reactions of CO and CO_2 with H_2 (Table 2, Eqs. (26), (28) and (29)). Within this range of temperature also a secondary reduction of CoO with H_2 takes place (Table 2, Eq. (7)) resulting in formation of H_2O as it was stated earlier [8].

The influence of the type of a crucible on the course of the III stage of HACOT decomposition is presented in Fig. 10. At a temperature > 300 °C the intensities of the MS curves for $m/z = 2$, 28 and 44 registered during the decomposition in the quartz crucible differs significantly from those taken in Pt and alox crucibles. The reactions between the solid phase and a self-generating gas phases and gas–gas phase reactions are favoured by the thicker layer of decomposed solid what is a case in Pt and alox crucibles (see Table 2, Eqs. (5), (8), (9), (11), (14) and (21)).

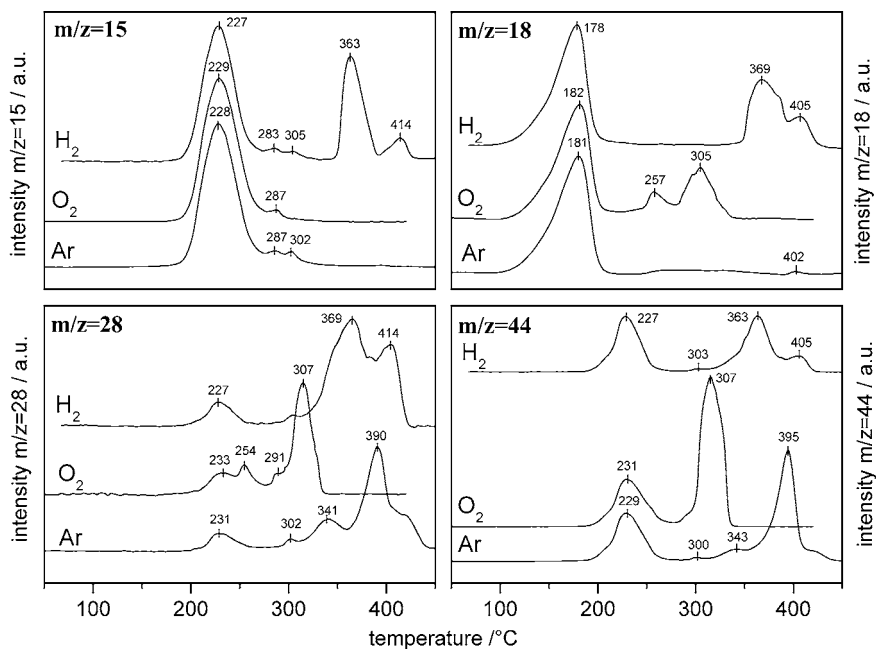


Fig. 5. Mass spectrometric signals recorded during decomposition of $[\text{Co}(\text{NH}_3)_6]_2(\text{C}_2\text{O}_4)_3 \cdot 4\text{H}_2\text{O}$ in platinum crucible in argon, 20 vol.% H_2 , balance Ar and 20 vol.% O_2 , balance Ar.

Table 1

TG and DTA results of the decomposition of $[\text{Co}(\text{NH}_3)_6]_2(\text{C}_2\text{O}_4)_3 \cdot 4\text{H}_2\text{O}$ in different gas atmospheres and different crucibles ($m \approx 72.4$ mg; heating rate 5°C min^{-1})

No.	Atmosphere (crucible)	Stage	Temperature range ($^\circ\text{C}$)	DTA _p	Mass loss (%)		Residue
					Observed	Theoretical	
1	Argon (platinum)	I	93–196	181 _{endo}	11.2	10.9	$[\text{Co}(\text{NH}_3)_6]_2(\text{C}_2\text{O}_4)_3$
		IIa	196–285	229 _{endo}	52.1	52.8	$\text{CoC}_2\text{O}_4 \cdot 1/2\text{NH}_3$
		IIb	285–330	285 _{endo}	55.3	55.3	CoC_2O_4
		III	330–450	303 _{exo} 336 _{endo} 394 _{endo}	80.0	79.6	$\text{Co} + \text{CoO}$
2	Argon (quartz)	I	88–177		10.9	10.9	$[\text{Co}(\text{NH}_3)_6]_2(\text{C}_2\text{O}_4)_3$
		II	177–291		53.9	55.3	CoC_2O_4
		III	291–420		79.7	79.6	$\text{Co} + \text{CoO}$
3	20 vol.% O_2 , balance Ar (platinum)	I	97–198	181 _{endo}	11.7	10.9	$[\text{Co}(\text{NH}_3)_6]_2(\text{C}_2\text{O}_4)_3$
		II	198–276	230 _{endo}	51.6	52.8	$\text{CoC}_2\text{O}_4 \cdot 1/2\text{NH}_3$
		III	276–348	315 _{exo}	74.4	75.6	Co_3O_4
4	20 vol.% O_2 , balance Ar (quartz)	I	76–178		10.9	10.9	$[\text{Co}(\text{NH}_3)_6]_2(\text{C}_2\text{O}_4)_3$
		II	178–278		53.8	55.3	CoC_2O_4
		III	278–330		74.6	75.6	Co_3O_4
5	20 vol.% H_2 , balance Ar (platinum)	I	85–196	179 _{endo}	11.4	10.9	$[\text{Co}(\text{NH}_3)_6]_2(\text{C}_2\text{O}_4)_3$
		IIa	196–279	228 _{endo}	51.8	52.8	$\text{CoC}_2\text{O}_4 \cdot 1/2\text{NH}_3$
		IIb	279–329	282 _{endo}	55.1	55.3	CoC_2O_4
		III	329–450	303 _{exo} 339 _{endo} 351 _{exo} 403 _{endo}	80.9	82.1	Co
6	20 vol.% H_2 , balance Ar (quartz)	I	70–182		11.3	10.9	$[\text{Co}(\text{NH}_3)_6]_2(\text{C}_2\text{O}_4)_3$
		II	182–298		54.1	55.3	CoC_2O_4
		III	298–409		81.1	82.1	Co

Table 2

The values of the Gibbs energy $\Delta_r G$ and the heat of the reaction $\Delta_r H$ at 600 K for reactions which may possibly occur during HACOT decomposition (in kJ)

No.	Reaction	$\Delta_r G$	$\Delta_r H$	References
1.	$\text{CoC}_2\text{O}_4 \rightarrow \text{Co} + 2\text{CO}_2$	-67.4	32.4–98.4	[12–14]
2.	$\text{CoC}_2\text{O}_4 \rightarrow \text{CoO} + \text{CO} + \text{CO}_2$	-28.4	81.4–147.4	[12–15]
3.	$\text{CoC}_2\text{O}_4 + 2/3 \text{O}_2 \rightarrow 1/3\text{Co}_3\text{O}_4 + 2\text{CO}_2$	-293.5	204.5–270.6	[12–15]
4.	$\text{CoC}_2\text{O}_4 + 4/3\text{NH}_3 \rightarrow \text{Co} + 2\text{CO} + 2/3\text{N}_2 + 2\text{H}_2\text{O}$	-55.4	178.7–244.7	[12–15]
5.	$\text{CoC}_2\text{O}_4 + 2\text{NH}_3 \rightarrow \text{Co} + 1/2\text{N}_2 + 3/2\text{H}_2 + 2\text{CO}_2$	-83.3	-19.0–47.0	[12–15]
6.	$\text{CoO} + \text{CO} \rightarrow \text{Co} + \text{CO}_2$	-39.0	-49.0	[16]
7.	$\text{CoO} + \text{H}_2 \rightarrow \text{Co} + \text{H}_2\text{O}$	-22.5	-10.2	[16]
8.	$\text{CoO} + 2\text{NH}_3 \rightarrow \text{Co} + \text{H}_2\text{O} + 2\text{H}_2 + \text{N}_2$	-54.1	92.7	[16]
9.	$\text{CoO} + \text{NH}_3 \rightarrow \text{Co} + \text{H}_2\text{O} + 1/2\text{N}_2 + 1/2\text{H}_2$	-38.3	41.2	[16]
10.	$\text{CoO} + 1/6\text{O}_2 \rightarrow 1/3\text{Co}_3\text{O}_4$	-68.4	-34.5	[16]
11.	$\text{Co} + 1/2 \text{O}_2 \rightarrow \text{CoO}$	-191.6	-234.6	[16]
12.	$\text{Co} + 2/3\text{O}_2 \rightarrow 1/3\text{Co}_3\text{O}_4$	-226.1	-303.0	[16]
13.	$\text{NH}_3 + \text{CO} \rightarrow \text{C} + 1/2\text{N}_2 + \text{H}_2\text{O} + 1/2\text{H}_2$	-65.4	-83.2	[16]
14.	$\text{NH}_3 + \text{CO} \rightarrow \text{HCONH}_2$	-193.6	-7.3	[17]
15.	$2\text{NH}_3 + \text{CO}_2 \rightarrow (\text{NH}_2)_2\text{CO}$	-207.6	32.5	[17]
16.	$2\text{NH}_3 + \text{CO}_2 \rightarrow \text{N}_2 + \text{C} + 2\text{H}_2\text{O} + \text{H}_2$	-64.7	7.1	[16]
17.	$\text{NH}_3 + 3/4\text{O}_2 \rightarrow 1/2\text{N}_2 + 3/2\text{H}_2\text{O}$	-333.4 ^a	-315.8 ^a	[16]
18.	$\text{NH}_3 + \text{O}_2 \rightarrow 1/2\text{N}_2\text{O} + 3\text{H}_2\text{O}$	-273.8 ^a	-275.1 ^a	[16]
19.	$\text{NH}_3 + 5/4\text{O}_2 \rightarrow \text{NO} + 3/2\text{H}_2\text{O}$	-249.3 ^a	-225.4 ^a	[16]
20.	$\text{NH}_3 + 7/4\text{O}_2 \rightarrow \text{NO}_2 + 3/2\text{H}_2\text{O}$	-269.5 ^a	-283.5 ^a	[16]
21.	$\text{NH}_3 + 2\text{O}_2 \rightarrow \text{HNO}_3 + \text{H}_2\text{O}$	-256.1 ^a	-330.7 ^a	[16]
22.	$2\text{NH}_3 \rightarrow \text{N}_2 + 3\text{H}_2$	-9.5 ^a	99.8 ^a	[16]
23.	$\text{CO} + \text{H}_2\text{O} \rightarrow \text{CO}_2 + \text{H}_2$	-16.6	-38.9	[16]
24.	$\text{CO} + \text{H}_2 \rightarrow \text{H}_2\text{O} + \text{C}$	-49.6	-134.6	[16]
25.	$2\text{CO} \rightarrow \text{CO}_2 + \text{C}$	-66.1	-173.4	[16]
26.	$\text{CO}_2 + 3\text{H}_2 \rightarrow \text{C} + 2\text{H}_2\text{O}$	-33.0	-95.7	[16]
27.	$\text{C} + 2\text{H}_2 \rightarrow \text{CH}_4$	-22.9	-83.3	[16]
28.	$\text{CO} + 3\text{H}_2 \rightarrow \text{CH}_4 + \text{H}_2\text{O}$	-72.5	-218.0	[16]
29.	$\text{CO}_2 + 4\text{H}_2 \rightarrow \text{CH}_4 + 2\text{H}_2\text{O}$	-55.9	-179.0	[16]
30.	$\text{C} + 1/2\text{O}_2 \rightarrow \text{CO}$	-164.5	-110.2	[16]
31.	$2\text{CO}_2 + 7\text{H}_2 \rightarrow \text{C}_2\text{H}_6 + 4\text{H}_2\text{O}$	-41.0	-288.8	[16]
32.	$2\text{CO} + 5\text{H}_2 \rightarrow \text{C}_2\text{H}_6 + 2\text{H}_2\text{O}$	-74.1	-366.5	[16]
33.	$\text{CO} + 1/2\text{O}_2 \rightarrow \text{CO}_2$	-230.6	-283.6	[16]

^a $T = 500 \text{ K}$.

The results of qualitative MS analysis presented above do not allow verifying univocally the assumed sequences of HACOT decomposition. It is still ambiguous whether N_2 and/or CO evolve as primary products in second stage because all three gases, i.e. CO_2 , N_2 and CO can contribute to the intensity of MS signal $m/z = 28$. To elucidate this problem the investigation of the composition of the gas phase by the FT-IR method as well as quantitative determination of the gas products by the PTA[®]-MS method were carried out.

3.3. Thermodynamics

The calculated values of the Gibbs energy, $\Delta_r G$, and enthalpy of the reaction, $\Delta_r H$ (using the literature data of the Gibbs energy and enthalpy of formation [12–17]) are listed in Table 2. The thermodynamic data presented in Table 2 of possible primary and secondary reactions indicate that some of these reactions under equilibrium conditions may take place within the temperature range of HACOT decomposition. However, some of these reactions can be hindered for kinetic reasons. Therefore theoretical possibility of their occurrences has to be confirmed experimentally, what is difficult without quantification of the mass spectrometric signals. This was done by PulseTA[®] technique [9].

3.4. Determination of gaseous products by FT-IR

Gaseous products evolved during the thermal decomposition of HACOT in helium detected by FT-IR are listed in Table 3. Evolved gas profiles compared with references [18–23] show clearly that NH_3 and CO_2 are evolved in the second stage of HACOT decomposition (173–232 °C) while CO and CO_2 in the third stage (277–314 °C). In the first stage only H_2O is liberated. As it can be seen the results are in agreement with those obtained by the MS method and prove the main primary gas products are H_2O (stage I), NH_3 (end of the first stage, the second stage), CO_2 (stage I/II and stage III) and CO (only stage III). The results support the assumed sequences of decomposition, i.e. Eqs. (5), (9), (10), (14) and exclude Eqs. (6) and (12).

3.5. Quantitative analysis of gaseous products by PulseTA[®]-MS

3.5.1. Water

The shape of the $m/z = 18$ signal and the continuous shift of the TG curve (Figs. 1, 3–10) indicate that, independently of the atmosphere and the crucible type, evolution of the crystallised water is not completed before the beginning of the

Table 3
Gaseous products evolved during decomposition of $[\text{Co}(\text{NH}_3)_6]_2(\text{C}_2\text{O}_4)_3 \cdot 4\text{H}_2\text{O}$ determined by FT-IR

Temperature range (°C)	Stage	Wave number (cm^{-1})	Assignments	References
100–190	I	4000–3750	H_2O	[18,19] [18,19,22]
		3750–3500	H_2O	
		1900–1590	H_2O	
		1550–1280	H_2O	
170–280	II	3750–3700	CO_2	[21]
		3750–3600	H_2O	[18,19,23]
		3650–3150	NH_3 , CO_2 , H_2O	[18–21,23]
		2400–2250	CO_2	[18,21–23]
		1800–1350	NH_3	[18–20,22]
		1600–1500	H_2O	[23]
		1250–720	NH_3 , CO_2	[18–21]
285–320	III	3750–3550	CO_2 , H_2O	[18,21]
		2400–2250	CO_2	[18,21,22]
		2250–2100	CO	[18,21–23]
		1630–1590	H_2O	[18–20]

second stage of HACOT decomposition. To determine the total amount of crystallised water the signals of TG and $m/z = 18$ were compared. The results presented in Table 4 indicate that independently of the kind of the gas atmosphere

and the crucible type the determined mass loss caused by the water evolving is equal to ca. 11 wt.% what is equivalent to 4 mol H_2O per mol HACOT and agrees well with the composition of the title compound. The results confirm the

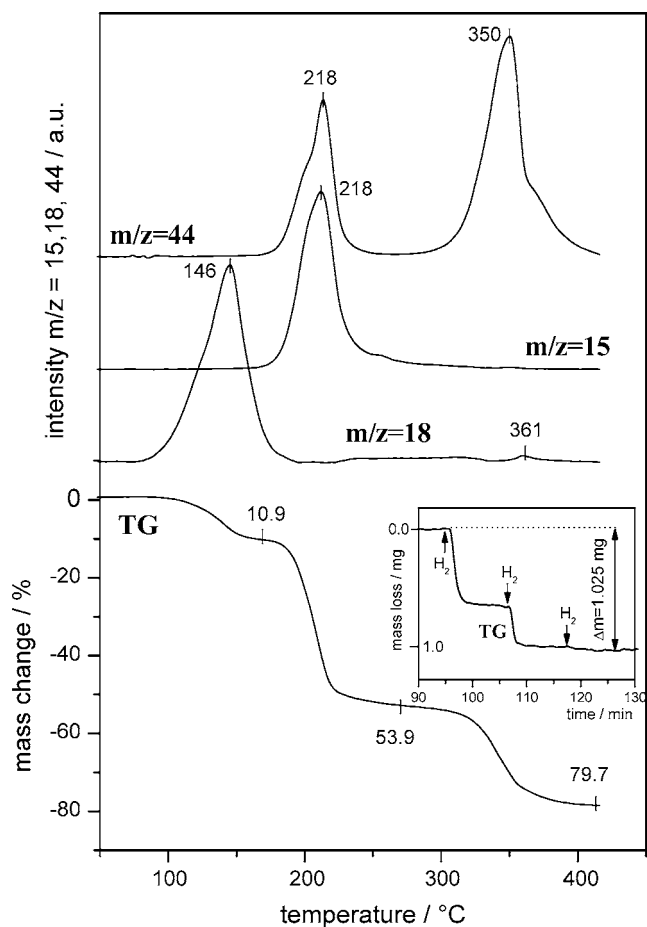


Fig. 6. Decomposition of $[\text{Co}(\text{NH}_3)_6]_2(\text{C}_2\text{O}_4)_3 \cdot 4\text{H}_2\text{O}$ in argon, quartz crucible.

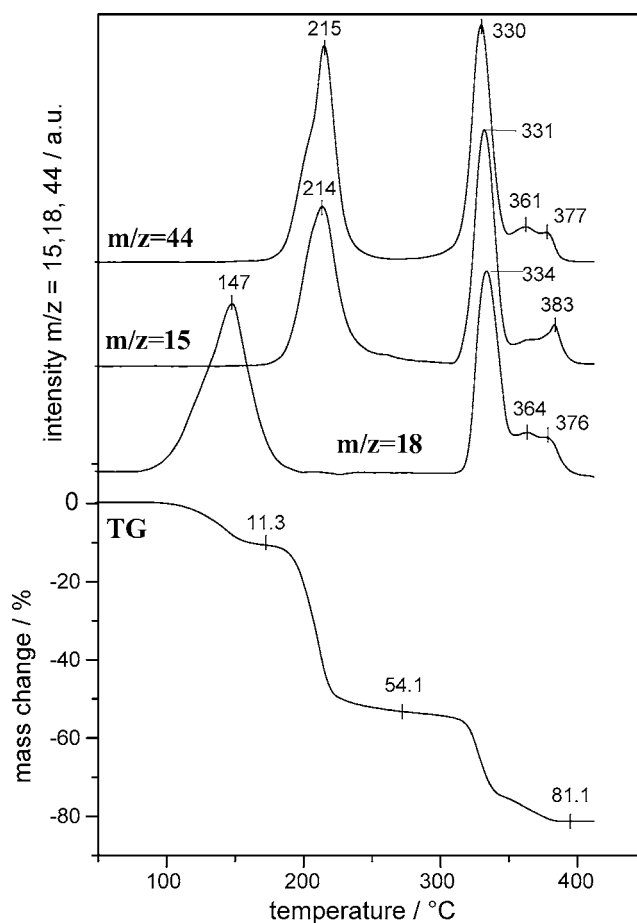


Fig. 7. Decomposition of $[\text{Co}(\text{NH}_3)_6]_2(\text{C}_2\text{O}_4)_3 \cdot 4\text{H}_2\text{O}$ in hydrogen (20 vol.%, balance Ar), quartz crucible.

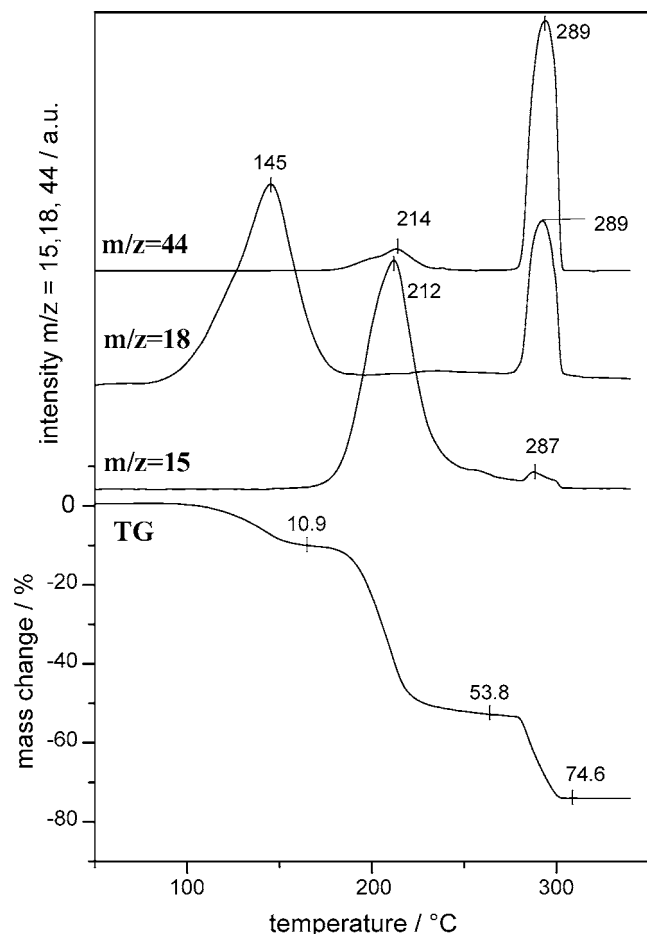


Fig. 8. Decomposition of $[\text{Co}(\text{NH}_3)_6]_2(\text{C}_2\text{O}_4)_3 \cdot 4\text{H}_2\text{O}$ in oxygen (20 vol.%, balance Ar), quartz crucible.

dehydration is the only reaction occurring during the first step of HACOT decomposition (Eq. (2)) independently of the experimental conditions.

In all atmospheres, independently of the type of crucible, some small amount of the water is clearly detectable in the gaseous products of the II and III stages. The least of the water (about 0.2–0.3 mol H_2O per mole HACOT) was registered in the inert atmosphere, more in the oxidising (0.5–1.7 mol H_2O per mol HACOT) and the most in the reducing atmosphere (2.4–2.9 mol H_2O per mol HACOT, third stage). In the oxidising atmosphere most of the water was registered during the HACOT decomposition in the Pt crucible what suggests their formation during NH_3 oxidation (Table 2, Eqs. (17)–(21), Figs. 4, 5 and 9) catalysed by Pt. The water was also formed due to secondary reaction of the formation of hydrocarbons as, e.g. methane in the reactions of CO_2

Table 4
The amount of crystallised water (wt.%) determined by TG–MS

Crucible (atm)	Ar	20 vol.% O_2	20 vol.% H_2
Alox	11.1	11.1	11.0
Quartz	11.0	11.0	10.9
Pt	10.9	10.9	11.0

or CO (the primary gaseous product of HACOT decomposition) with H_2 catalysed by freshly formed Co_{met} (Table 2, Eqs. (28), (29), (31) and (32)). The experimental proof of the CH_4 formation in H_2 and/or Ar (in smaller extent) atmosphere during decomposition of cobalt oxalate (third stage of HACOT decomposition) was given in [8].

3.5.2. Ammonia

The quantitative data for NH_3 listed in Table 5 obtained by the quantification of the signal $m/z = 15$ show that the total amount of NH_3 liberated during HACOT decomposition is in the range of 9.5–10 mol NH_3 per mol reactant (79–83% stoichiometric content of NH_3). The influence of the crucible type in an inert atmosphere of the amount of detected ammonia (Table 5) is small. The apparently higher amount of NH_3 measured in the reducing atmosphere (Figs. 3, 5, 7 and 9) is caused by contribution of CH_4 to the intensity of $m/z = 15$ signal. Methane is the product of the secondary reactions (see Table 2, Eqs. (28) and (29)) in III stage of HACOT decomposition.

The determined amount of evolving NH_3 is in good agreement with the data published by Saito [24] for $[\text{Co}(\text{NH}_3)_6]_2(\text{SO}_4)_3 \cdot 5\text{H}_2\text{O}$ decomposition in Ar atmosphere (82% of stoichiometric amount of NH_3 was determined i.e. 9.8 mol NH_3 per mol compound). Moreover Saito considers that in the air missing ca. 2 mol NH_3 were oxidised. We tested experimentally the possibility of NH_3 dissociation under the conditions of HACOT decomposition and stated the dissociation did not occur over empty crucibles (see Fig. 12). The experiments with the decomposition of ammonia over metallic cobalt (not shown) indicate that the reaction starts at ca. 290 °C.

Our results presented in Fig. 12 show that NH_3 is oxidised in the atmosphere 20 vol.% O_2 . Above 200 (Pt crucible) and 270 °C (alox crucible) a clear oxidation of NH_3 to N_2 and to N_2O (decrease in the signal $m/z = 15$) occurs. At slightly higher temperatures NH_3 is oxidised also to NO ($m/z = 30$). It is clearly seen that oxidation of NH_3 is catalysed by platinum. At the temperatures mentioned above the signal $m/z = 18$ originated from H_2O (H_2O is the product of NH_3 oxidation, see Table 2, Eqs. (17)–(20) was also registered). The course of the signals $m/z = 15, 30, 44$ registered during passing of NH_3 pulses over an empty Pt crucible shows that ammonia is not oxidised in Ar. All these results (decomposition of ammonia over Co met, oxidation by oxygen and possibility of the secondary reactions as, e.g. 8, 9, Table 2) explain the fact that the amount of the detected ammonia is smaller than results from the stoichiometry of the title compound.

3.5.3. CO_2 and CO

Quantification of the signal $m/z = 44$ registered in the inert atmosphere shows that 5.2–5.5 mol CO_2 per mol compound is evolved within the whole range of HACOT decomposition temperatures: ca. 1.8–2.0 mol CO_2 is formed during II stage and ca. 3.5 mol during III stage (Table 6). Quantification of the signal $m/z = 28$ corrected by contribution

Table 5
The amount of the evolved NH_3 calculated by quantification of the signal $m/z = 15$ (mol NH_3 per mol HACOT)

Crucible	Argon		Oxygen		Hydrogen		
	Temperature range	mol evolved gas/mol complex	Temperature range	mol evolved gas/mol complex	Temperature range	mol evolved gas/mol complex	
Pt	161–346	9.9	177–335	9.3	167–393	12.0 ^a	
	161–275	9.1	177–280	9.0	167–329	8.4	
	275–346	0.8	280–335	0.3	340–393	3.6 ^a	
Quartz	160–370	9.8	159–303	10.1	165–402	15.6 ^a	
				155–278	10.0	165–306	7.9
				278–303	0.1	306–352	6.2 ^a
Alox	165–352	9.5			352–402	1.5 ^a	
	165–273	9.2					
	273–352	0.3					

^a Calculated on the assumption that the signal comes only from NH_3 (NH^+).

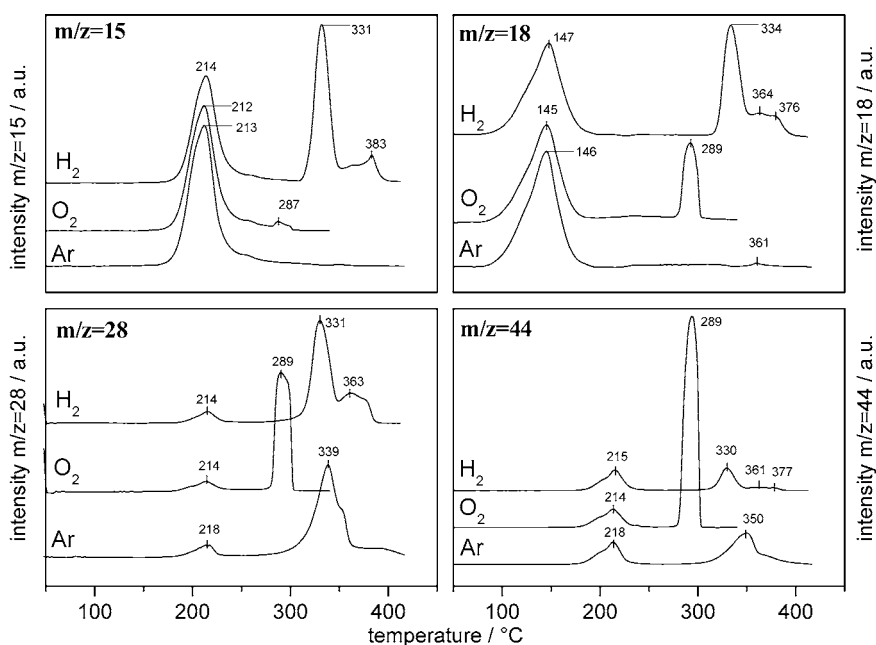


Fig. 9. Mass spectrometric signals recorded during decomposition of $[\text{Co}(\text{NH}_3)_6]_2(\text{C}_2\text{O}_4)_3 \cdot 4\text{H}_2\text{O}$ in thin layer in quartz crucible in argon, 20 vol.% H_2 , balance Ar and 20 vol.% O_2 , balance Ar.

Table 6
The amount of the evolved CO_2 calculated by quantification of the signal $m/z = 44$ (mol CO_2 per mole HACOT)

Crucible	Argon		Oxygen		Hydrogen	
	Temperature range	mol evolved gas/mol complex	Temperature range	mol evolved gas/mol complex	Temperature range	mol evolved gas/mol complex
Pt	165–454	5.2	177–348	5.7	174–429	4.0
	165–310	1.8	177–278	1.8	174–282	1.8
	310–454	3.4	278–348	3.9	291–429	2.2
Quartz	150–416	5.5	172–307	5.0	163–395	3.3
	150–259	2.0	172–257	1.6	163–259	1.7
	278–416	3.5	273–307	3.4	283–350	1.3
Alox					350–395	0.3
	180–447	5.5				
	180–277	1.9				
	310–358	0.4				
	358–447	3.2				

Table 7

The amount of the evolved mole CO per mol HACOT calculated by quantification of the signal $m/z = 28$ with subtracting the intensity of the CO_2 fragmentation (CO^+)

Crucible	Argon		Oxygen		Hydrogen	
	Temperature range	mol evolved gas/mol complex	Temperature range	mol evolved gas/mol complex	Temperature range	mol evolved gas/mol complex
Pt	191–454	0.9	180–348	0.2	177–262	0 ^a
	191–270	0 ^a	180–278	0		
	274–361	0.1	278–348	0.2		
	361–454	0.8				
Quartz	176–416	1.0	171–313	0.1	176–393	1.4
	176–244	0 ^a	171–240	0 ^a	176–244	0 ^a
	263–416	1.0	270–313	0.1	275–349	1.0
Alox	140–454	0.8			349–393	0.4 ^b
	140–268	0 ^a				
	310–358	0.2				
	358–454	0.6				

^a Only from the CO_2 fragmentation.

^b Calculated on the assumption that it originates only from CO^+ but within this range of temperature the signal comes probably also from the secondary reactions products, e.g. C_xH_y^+ .

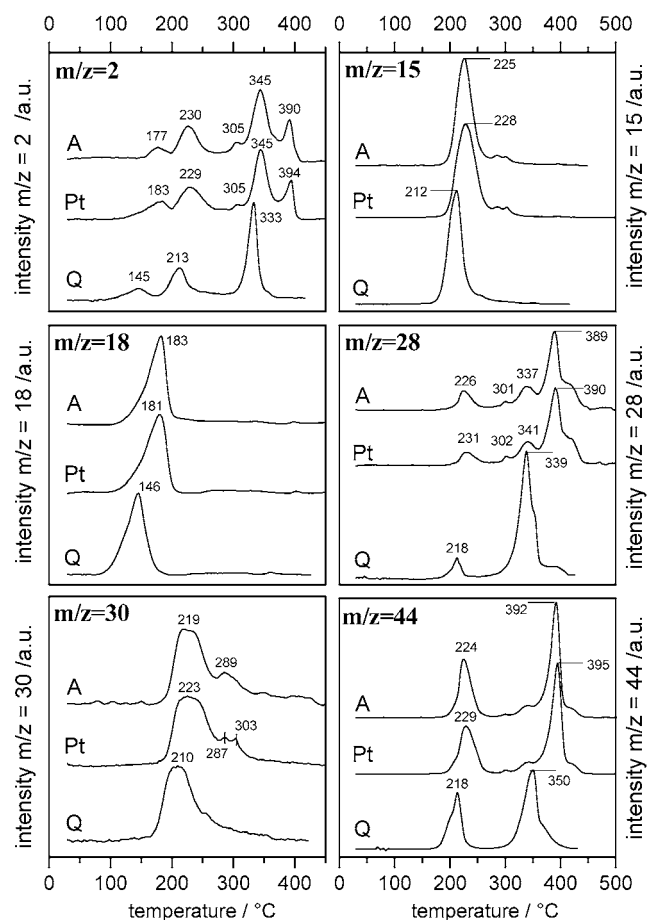


Fig. 10. Mass spectrometric signals recorded during decomposition of $[\text{Co}(\text{NH}_3)_6]_2(\text{C}_2\text{O}_4)_3 \cdot 4\text{H}_2\text{O}$ in argon in different crucibles: alox (A), platinum (Pt) and quartz (Q).

of the intensity of CO_2 fragmentation allowed to estimate the amount of CO released (Table 7). It was found that ca. 1 mol CO per mole HACOT was formed in Ar atmosphere in the third stage of decomposition. In the second stage CO was not detected what excludes one of the assumed sequences of the decomposition (Eqs. (6) and (12)). Instead, the data obtained for the third stage confirm the sequences of decomposition assumed for this stage, i.e. Eqs. (9) and (10). The absence of CO during the second stage of the decomposition was confirmed also by TA-FT-IR experiments (not shown).

In the oxidising atmosphere (Pt crucible) the total amount of CO_2 detected in third stage increases from 5.2 to 5.7 mol (Table 6) and the amount of CO decreases from 0.9 to 0.4 mol (Table 7) due to the oxidation (Table 2, Eq. (33)).

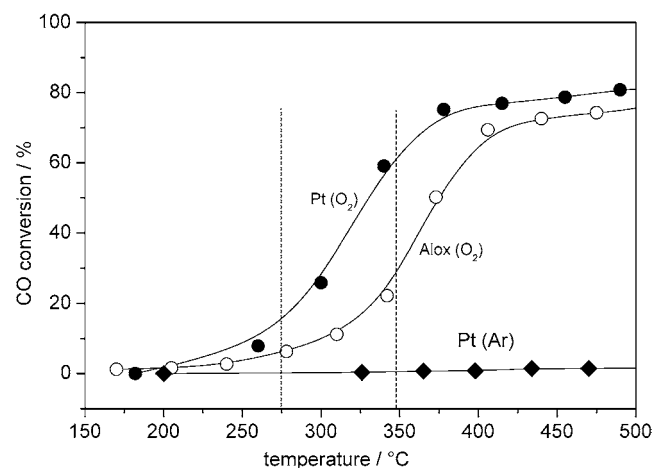


Fig. 11. CO conversion in oxygen and argon measured over empty platinum crucible in argon and over empty platinum and alox crucibles in 20 vol.% O_2 , balance Ar. The dotted lines indicate the temperature range of CO evolution during the third stage of $[\text{Co}(\text{NH}_3)_6]_2(\text{C}_2\text{O}_4)_3 \cdot 4\text{H}_2\text{O}$ decomposition.

This observation is in full agreement with the reference tests presented in Fig. 11 showing that at 450 °C ca. 78% CO reacts to CO₂. During HACOT decomposition in the quartz crucible and oxidising atmosphere only 8% CO released of the registered in the inert atmosphere (Table 7).

In order to investigate additionally the possibility of CO disproportionation in oxygen and argon under HACOT decomposition conditions pulses of CO were injected over empty platinum crucible in Ar and over empty Pt and alox crucibles in 20 vol.% O₂. The results presented in Fig. 11 show that in the temperature range characteristic for the third stage of HACOT decomposition the disproportionation of CO (Table 2, Eq. (25)) occurs only in a very small extent ($\leq 0.5\%$ CO) over the empty Pt crucible in Ar. However previously [8] it was revealed that the disproportionation clearly runs above 250 °C over Co_{met}, which catalyses this reaction. So, because in III stage of HACOT decomposition Co_{met} is formed, the Boudouard's reaction may also be expected. In the oxidising atmosphere conversion of CO into CO₂ occurs in significant extent and at 345 °C amounts to ca. 61% CO over Pt crucible or 29% CO over alox crucible. These results are in good agreement with the data listed in Table 7 where the estimated quantity of CO evolved during HACOT decomposition in oxidising atmosphere in Pt crucible is ca. 4.5 times lower than in Ar atmosphere.

In the reducing atmosphere the clearly less amount (of 1.2–2 mol) of CO₂ was detected than in argon (Table 6). This observation confirms the secondary reactions between the primary CO₂ and H₂ resulting in hydrocarbons formation, mainly CH₄, (Table 2, Eqs. (29) and (31)) revealed earlier [8].

4. Discussion

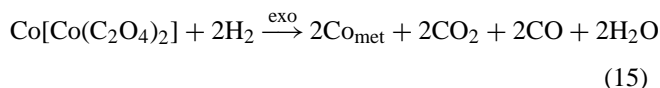
The TA–MS investigations of the gaseous products confirmed that among the products of HACOT decomposition in Ar atmosphere there are H₂O (I stage), NH₃, CO₂, maybe CO and the rest of crystallisation water (II stage), CO₂ and probably CO (III stage). Without quantification of MS signals it was difficult to conclude whether or not in the second stage of decomposition CO and N₂ evolve therefore corroboration or exclusion of Eqs. (6), (12) and (14) was impossible. This was due to the fact the signal $m/z = 28$ may originate from both, N₂⁺ ions and CO⁺, formed from CO and/or CO₂ and the signal $m/z = 14$ from N⁺ can be due to the fragmentation of NH₃ and/or N₂. The $m/z = 12$ cannot be used for proving CO evolution in this stage due to the presence of CO₂ having cracking pattern $m/z = 12$ with relative intensity of ca. 10. However the investigation of the composition of the gas products by FT-IR shown undoubtedly that CO is not evolved in the second stage. It makes possible to exclude the sequence (6) (II stage) and Eq. (12) (substage IIa). So the sequence (14) (simultaneous evolving of NH₃ and CO₂) seems to describe the whole second stage. Simultaneous liberation of CO and CO₂ was found in the III stage what confirms the reality of the assumed sequences (9) and (10).

The quantitative PTA[®]–MS studies of HACOT decomposition gas products in Ar corroborate that in the I stage and at the beginning of II stage the whole amount of crystallised water is liberated, i.e. 4 mol H₂O/mole HACOT what additionally proves Eq. (2) and/or Eq. (5). Also the amount of CO liberated in III stage (≤ 1 mol per mole HACOT) as well as the amount of CO₂ (ca. 3.5 mol per mole HACOT) confirm the assumed sequences (9) and (10). The amount of CO₂ determined in II stage equal to 1.8–2.0 mol per mole HACOT supports the assumed sequence (14). Some small differences in the amounts of the above-mentioned products detected during the HACOT decomposition in different crucibles result from numerous secondary reactions.

The determined total amount of NH₃ liberated during HACOT decomposition in Ar is equal to 9.5–9.9 mol NH₃ per mol HACOT. The title compound contains 12 mol NH₃ thus the lack of ca. 2 mol NH₃ must result from some secondary reactions in which NH₃ is consumed occurring over 280 °C (see mass loss stage II, Table 1). They are: (i) CoO reduction by NH₃ (Table 2, Eqs. (8) and (9)) in which H₂ and H₂O are produced and (ii) NH₃ dissociation over Co_{met}.

Under the oxidising as well as reducing atmospheres the influence of secondary reactions on the composition of both, solid and gaseous products is more distinct and appears particularly strongly during the III stage. In the oxidising atmosphere Co₃O₄, the solid product of decomposition, in fact is formed in a secondary reaction by oxidising the primary product i.e. the mixture of Co + CoO. Very low (0.1–0.2 mol per mole HACOT) CO content together with a high CO₂ (5.1–5.7 mol) concentration and results of test studies of CO behaviour in the oxidising atmosphere (Fig. 11) confirm the summary equation (8) proposed for description of the third stage. In Eq. (14) describing the stoichiometry of the second stage the coefficient of NH₃ equal to 12 ought to be replaced by (12 – *n*) where *n* represents part of NH₃ consumed in the secondary reactions. In the oxidising atmosphere one can find the products of NH₃ oxidation namely N₂ (maximum of oxidation at 250 °C), N₂O (maximum of oxidation at 285 °C) and NO (maximum of oxidation at 530 °C), see Fig. 12. The lack of water among the gas products of the decomposition in reducing atmosphere (Figs. 3 and 7) within the range 250–320 °C suggests that H₂O which is liberated within this range of temperature in 20 vol.% O₂ (Fig. 4) is produced by NH₃ oxidation.

In the reducing atmosphere the only identified solid product is Co_{met}. In fact this is a secondary product resulting from reducing the primary product (mixture of Co_{met} and CoO) by hydrogen. Because of that the sequence of Eqs. (9) and (15) resulting in overall Eq. (16) describe the third stage of HACOT decomposition:



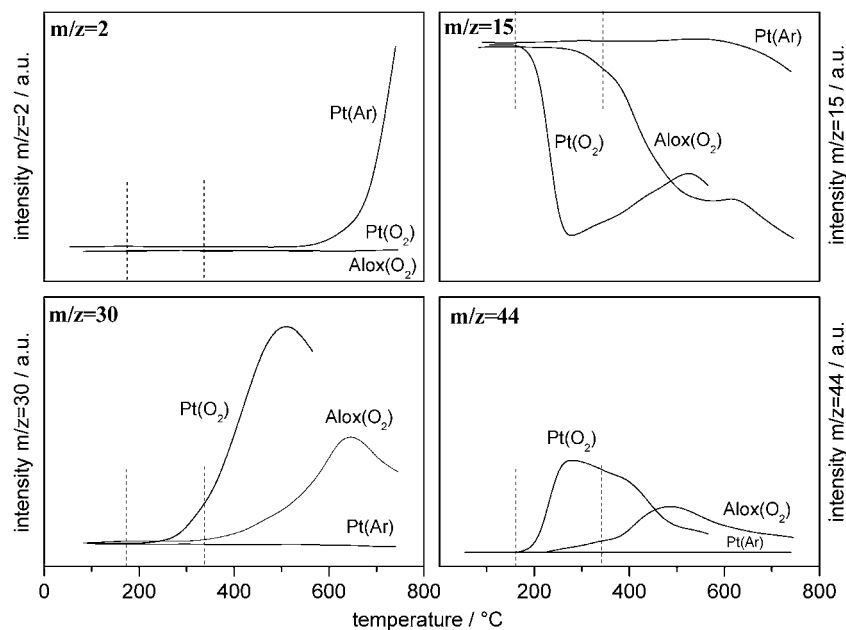
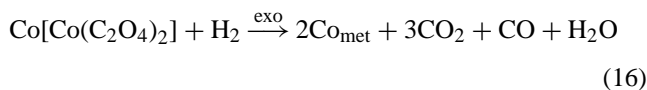


Fig. 12. Mass spectrometric signals recorded during injection of 2 ml NH_3 over empty platinum crucible in argon and over empty platinum and alox crucibles in 20 vol.% O_2 , balance Ar. The dotted lines indicate the temperature range of NH_3 evolution during the second stage of $[\text{Co}(\text{NH}_3)_6]_2(\text{C}_2\text{O}_4)_3 \cdot 4\text{H}_2\text{O}$ decomposition.

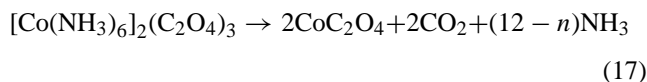


The main gaseous products of III stage in the reducing atmosphere are CO_2 , CO and H_2O , however their amounts 1.6–2.2, ca.1.5 and 2.4–2.9 mol CO_2 per mol HACOT differ from those expressed by the stoichiometry of the reaction (15). This finding confirms the occurrence of the secondary reactions (24, 26–29, 31, 32, Table 2) during the decomposition in the reducing atmosphere resulting in formation of H_2O , and hydrocarbons (mainly CH_4).

To sum up the above we propose that three main consecutive steps of HACOT decomposition are described best by the equations:

Stage I (argon, hydrogen, air)—Eq. (5).

Stage II (argon, hydrogen, air):



where n denotes the amount of NH_3 consumed in secondary reactions.

Stage III (argon)—Eqs. (9)–(11). Stage III (hydrogen)—Eq. (16).

Stage III (air)—Eq. (8).

Besides these main reactions a lot of secondary reactions occur which influence strongly the shape of the registered TG–DTA curves and the composition and amount of gaseous and solid products. The results presented above and their discussion show irrefutably that, as in Ref. [8], drawing a conclusion concerning the decomposition on the basis of

results of thermogravimetry and differential thermal analysis only often leads to erroneous deductions. Even the studies by TG–DTA–MS methods may be insufficient for determining the course of multistage decomposition when the gaseous and solid products can react in the secondary reactions. In such a case the investigation needs application of the simultaneous techniques such as TA–MS or TA–FT-IR combined with the method allowing quantification of spectroscopic signals such as pulse thermal analysis (PTA[®]) which additionally allows investigation of gas–solid and gas–gas reactions in situ.

References

- [1] E. Ingier-Stocka, M. Maciejewski, *Thermochim. Acta* 354 (2000) 45–57.
- [2] W.W. Wendlandt, J.P. Smith, *The Thermal properties of Transition–Metal Amine Complexes*, 43, Elsevier, Amsterdam, 1967, pp. 37–103, 43.
- [3] F. Paulik, *Special Trends in Thermal Analysis*, Wiley, Chichester, 1995, p. 384.
- [4] E. Ingier-Stocka, A. Bogacz, *J. Therm. Anal.* 35 (1989) 1373–1386.
- [5] W. Hadrich, *Dissertation*, Eberhard-Karls-Universitaet zu Tubingen, 1979.
- [6] G.L. Jeyaraj, J.E. House Jr., *Thermochim. Acta* 68 (1983) 201–206.
- [7] L.W. Collins, W.W. Wendlandt, *Thermochim. Acta* 8 (1974) 315–323.
- [8] M. Maciejewski, E. Ingier-Stocka, W.-D. Emmerich, A. Baiker, *J. Therm. Anal. Calorim.* 60 (2000) 735–758.
- [9] M. Maciejewski, C.A. Muller, R. Tschan, W.-D. Emmerich, A. Baiker, *Thermochim. Acta* 295 (1997) 167–182.
- [10] M. Maciejewski, A. Baiker, *Thermochim. Acta* 295 (1997) 95–105.
- [11] J. Bjerrum, J.P. McReynolds, *Inorg. Synth.* 29 (1946) 220.
- [12] V.P. Glushko, V.A. Medvedeva (Eds), *Termicheskie Konstanty Veshestv*, vol. 6, Part I, AN SSSR and VINITI, Moscow, 1972, p. 254.

- [13] A. Coetzee, D.J. Eve, M.E. Brown, *J. Therm. Anal.* 39 (1993) 947–973.
- [14] R.C. West (Ed.), *Handbook of Chemistry and Physics*, 64th ed., CRC Press, Florida, 1984, p. D-66.
- [15] V. My Le, G. Perinet, *Bull. Soc. Chim. France* 10 (1969) 3421–3427.
- [16] I. Barin, *Thermochemical Data of Pure Substances*, VCH, 1989.
- [17] Outokumpu HSC Chemistry[®] for Windows, Version 4.0, 1999.
- [18] K. Nakamoto, *Infrared and Raman Spectra of Inorganic and Coordination Compounds*, 4th ed., Wiley, New York, 1986, pp. 106, 112, 115, 118.
- [19] K. Jones, *The Chemistry of Nitrogen*, *Comprehensive Inorganic Chemistry*, Pergamon Press, Oxford, 1975, Chapter 19, p. 209.
- [20] G.C. Pimentel, M.O. Bulanin, M. Van Thiel, *J. Chem. Phys.* 36 (1962) 500–506.
- [21] K.E. Dierenfeld, *J. Chem. Ed.* 72 (3) (1995) 281–283.
- [22] S.B. Warrington, in: E.L. Charsley, S.B. Warrington (Eds.), *Evolved Gas Analysis, in Thermal Analysis—Techniques and Applications*, The Royal Society of Chemistry, 1992, p. 84.
- [23] S.R. Naidu, N.M. Bhide, K.V. Prabhakaran, E.M. Kurian, *J. Therm. Anal.* 44 (1995) 1449–1462.
- [24] A. Saito, *Thermochim. Acta* 177 (1991) 197–212.